Solid State Science and Technology, Vol. 20, No 1 & 2 (2012) 68-74
ISSN 0128-7389

EFFECT OF OXYGEN ADDITION ON SIDEWALLS OF SILICON SQUARE MICRO-PIT ARRAYS USING SF_6 BASED REACTIVE ION ETCHING

Maryam Alsadat Rad* and Kamarulazizi Ibrahim

Nano Optoelectronics Research & Technology Lab, School of Physics, Universiti Sains Malaysia, 11800 USM, Penang, Malaysia

**Corresponding author: maryam.s.rad@gmail.com*

ABSTRACT

In this paper, the etching profile of silicon square micro-pits array using SF_6 based Reactive ion etching (RIE) is reported. This micro-pits array was created on a Si substrate with poly methyl methacrylate (PMMA) mask during the RIE process. Effects of O_2 addition and pressure decreasing were described by chemical reactions of etching and experimental results. Atomic force microscopy (AFM) was utilized to investigate etching profile of these micro-pit arrays. Etching of micro-pits with O_2 addition results a vertical sidewall with 3 nm roughness of the inter-pit spacing, while V-groove shaped in sidewall was obtained in absence of O_2. These square micro-pits have a good potential to be used in biology applications due to its dimension, especially for confinement region for biological objects e.g. DNA.

Keywords: Silicon; Micro-pit; Reactive ion etching; Sidewall; Electron beam lithography

INTRODUCTION

Micro and nano-pit (hole) arrays of metal [1] and semiconductors [2] have been utilized in many applications. They are of great interest due to a wide variety of applications which employed as the building blocks of photonic crystals [3, 4], the microfluidic fractionation devices of molecules [5, 6], nanoscale biosensing [7], the molds of nanoimprint lithography [8], and other novel devices in biological and physical sciences.

Anisotropy, roughness and smoothness are the major features that are concerned in the characterization of micro-pits or holes fabrication. Controlling etching profile is an important factor in any silicon etching process. Vertical sidewalls are desirable in the fabrication of MEMS sensors and actuators [9, 10]. Normally, slightly U-shaped sidewalls are required with smooth surface for device application.

Plasma chemistry is one of the crucial factors to determine the micro-pits sidewall shape. The fluorine-based plasmas such as SF_6-based [11, 12] are more attractive than chlorine-based plasmas [13, 14] and bromine-based plasmas [15] for anisotropic etching

of Si micro-pits and trenches. In SF_6 plasma etching, an isotropic etching profile is created due to the fact that F atoms etch silicon spontaneously. Anisotropic etching and high etch rates have been demonstrated in RIE plasmas containing SF_6 and O_2 [16, 17]. Most of the fabricated micro-pits have circular shape and there are limited literatures on fabricating of square micro-pits which can be used in biochips.

In this work, we have investigated the etching profile of Si micro-pits arrays during SF_6 plasma etching with PMMA mask. Chemical explanations of the O_2 addition effect to SF_6 plasma etching are provided for anisotropic micro-pits etching of silicon. The experimental results show that by decreasing the pressure, passivation layer protect the sidewall from etching and will make it anisotropic. The AFM is used to show the etching profile of silicon micro-pit.

EXPERIMENTAL PROCEDURES

In this work, p-type silicon (100) was cleaned in a wet chemical etch process (standard cleaning processes), using RCA cleaning method in order to desorb ionic and heavy metal atomic contaminants and remove native oxide. After that 300 nm thick poly methyl methacrylate (PMMA) 950K (% 4A) layer was coated on 1cm×1cm Si wafer. In order to get the pits around 1×1 μm^2 in size, a Raith 150 EBL tool has been used to drill micro-pit arrays of square and tilted pattern. The exposed PMMA area were developed in 1:3 MIBK:IPA for 30 s. It is followed by post baking of sample at 100 $^{\circ}$C for 2 min. The remaining PMMA on the Si substrate serves as mask for the reactive ion etching (RIE) process. In this process, RIE facility (Oxford Instruments, PlasmaLab 80 RIE) has been utilized in order to fabricate the Si micro-pit with SF_6 and O_2 etchants.

RESULTS

Figure 1(a) and (b) show two SEM images of the ordered square and tilted micro-pits arrays around 1×1 μm in size on Si substrate after developed PMMA area for 30 s, respectively.

Figs 2 (a) and (b) displays the SEM images of silicon square and tilted micro-pits arrays after RIE process and PMMA removal, respectively. The tilted micro-pit array was etched by SF_6 and O_2, while the square micro-pit array was etched just with SF_6.

In Figure 3, AFM images of square micro-pits arrays are shown. The 3D topography of array is shown in Figure 3(a) in 10×10 μm^2 field. The depth of micro-pits is about 100 nm, as shown in etching profile in Figure 3(b). The surface of fabricated arrays can be seen in Figure 3(b) in a 10×10 μm^2 filed size. The V-groove shape of micro-pits are clear in the Figure 3(c) and show the quality of etching processes to get Si micro-pits arrays.

Solid State Science and Technology, Vol. 20, No 1 & 2 (2012) 68-74
ISSN 0128-7389

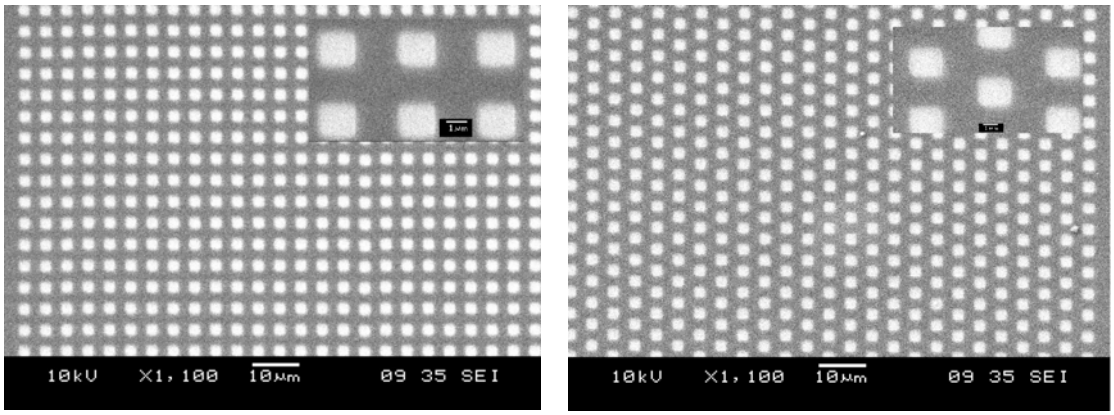

(a) (b)

Figure 1: The generated micro-pits pattern on PMMA using electron beam lithography (a) for square array and (b) tilted arrays. The insets show the high resolution of patterns

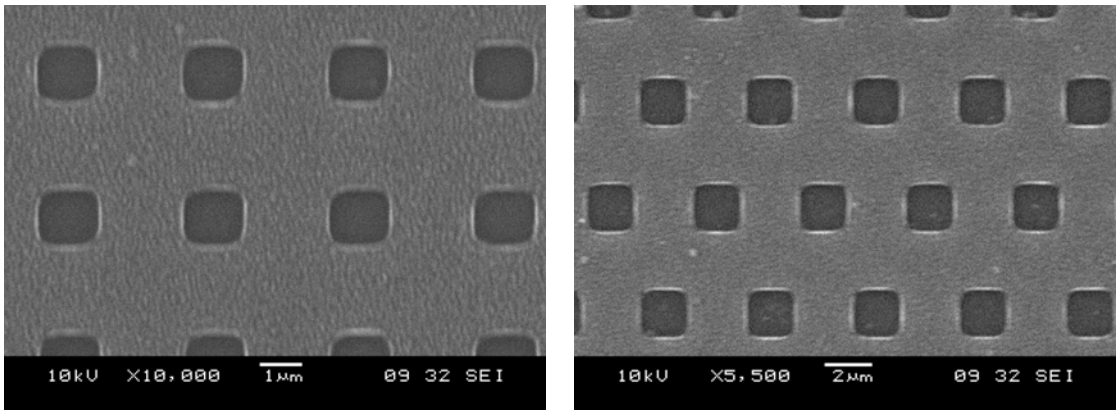

(a) (b)

Figure 2: Displays the SEM images of silicon micro-pits arrays after RIE process (a) for square array and (b) for tilted array

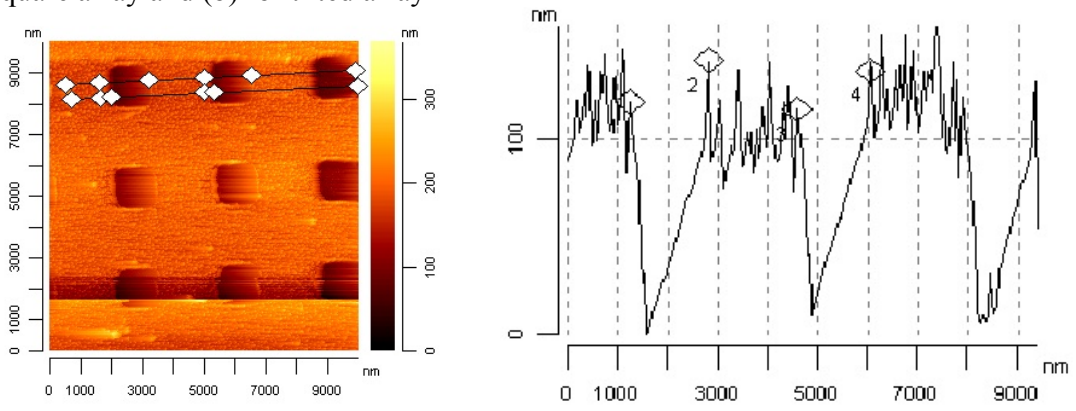

(a) (b)

Figure 3: (a) 3D topography of fabricated Si micro-pit array, (b) Etching profile of Si micro-pits arrays and (c) the 2D surface image of Si micro-pits arrays

Solid State Science and Technology, Vol. 20, No 1 & 2 (2012) 68-74
ISSN 0128-7389

In Figure 4, AFM images of square micro-pits arrays are shown. The 3D topography of array is shown in Figure 4(a) in 16×16 μm^2 field size which the roughness of the inter-pit spacing is less than 3 nm (~2.56 nm). The surface of fabricated arrays can be seen in Figure 4(b) in a 16×16 μm^2 filed size. The depth of micro-pits is about 120 nm, as shown in etching profile in Figure 4(c). The vertical shape of micro-pits are clear in the Figure 4(c) and show the quality of etching processes to get Si micro-pits arrays.

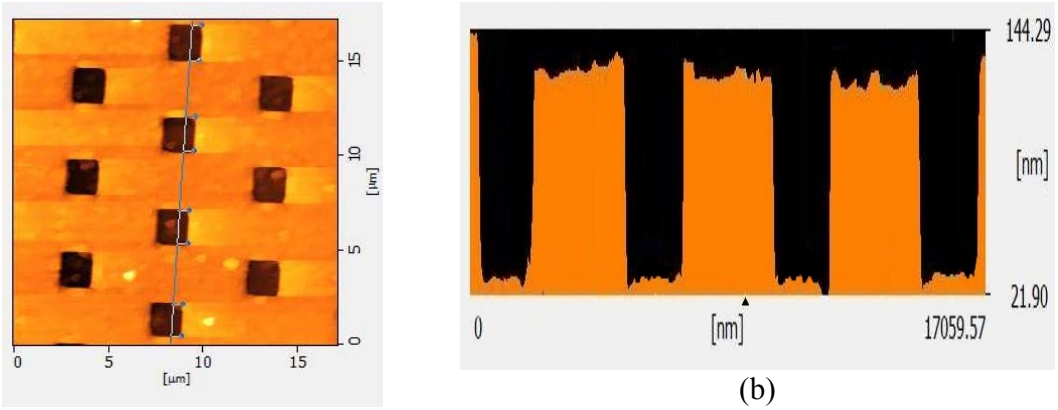

(a) (b)

Figure 4: (a) 3D topography of fabricated Si micro-pit array, (b) Etching profile of Si micro-pits arrays and (c) the 2D surface image of Si micro-pits arrays

DISCUSSION

In our work, SF_6 based plasma etchants is selected for RIE etching of silicon micro-pits arrays. The mentioned used gasses, SF_6 and O_2, generate F^* and O^* free radical under the influence of strong electric fields generated in the reactive ion etcher, as shown in Eq. (1) and (2). According to Eq. (3), the F^* radicals initiate a chemical reaction with silicon, producing the highly volatile by product SiF_4.

$$SF_6 + e \rightarrow SF_x + 4F^* + e \quad (x \leq 5) \qquad (1)$$
$$O_2 + e \rightarrow 2O^* + e \qquad (2)$$
$$Si + 4F^* \rightarrow SiF_4 \qquad (3)$$
$$Si + 2O^* \rightarrow SiO_2 \qquad (4)$$
$$SiO^2 + 4F^* \rightarrow SiF_4 + O_2 \qquad (5)$$

According to Eq. (6), the O^* radicals act to passivate the silicon surface by forming SiO_xF_y (silicon oxyfluoride). At the bottom of pit the SiO_xF_y layer is very thin due to intensive ion bombardment. The schematic of this etching process is shown in Figure 5.

$$SiF_4 + O_2 \rightarrow SiO_xF_y \qquad (6)$$

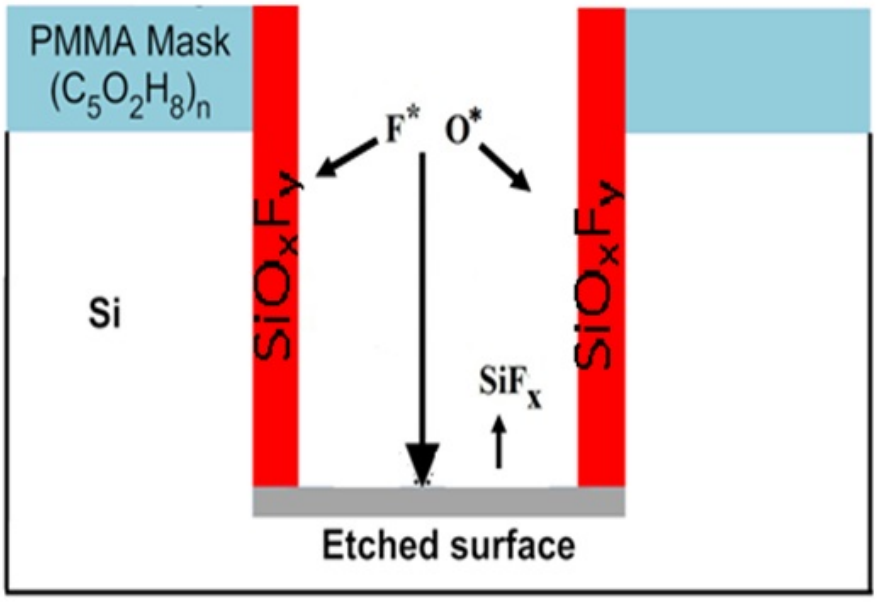

Figure 5: Schematic representation of micro-pit etching in SF_6 and O_2 plasma

At lower system pressures (10 mtorr), fewer reactive ions exist within the chamber at any one time, resulting in fewer collisions and fewer chances for poorly directed ions to cause lateral etching and make anisotropic sidewall as you can see in Figure 4(c).

At very high oxygen concentrations, the silicon etch rate is retarded due to polymerization on the side walls and bases of etch trenches. The polymers protect the silicon from reaction with F* radicals, thereby, causing a decrease in silicon etch rate with further increases in oxygen concentration [18-20]. In fact according to equation (5) for too much O_2, silicon look like SiO_2 and etch rate of SiO_2 is less than silicon.

At low oxygen concentrations (10 sccm) that we used in this work, the oxygen reacts with fluorosulfuric (SF_x) radicals, thereby hindering their reaction with F^* radicals and the subsequent reformation of sulfur hexafluoride (SF_6). These reactions are shown in Eqs. (7) and (8).

$$SF_x^+ + O_2 \rightarrow SO_2F_2 + F(x\text{-}2) \qquad (x \leq 5) \qquad (7)$$

$$SF_x^+ + F^* \rightarrow SF_{x+1} \qquad (x \leq 5) \qquad (8)$$

The result is a net increase in the concentration of fluoride radicals, leading to an increase in the silicon etch rate around 120 (nm) as shown in the etch profile of silicon in Figure 4 (c). There is a constant competition between the fluorine radicals that etch and oxygen radicals that passivate the silicon. Therefore, a certain concentration of O_2 is to be added to SF_6 to achieve a balance between the oxygen and fluorine radicals to

achieve vertical sidewalls. Meanwhile, PMMA etching rate increases by increasing the O_2 flow rate [21]. So, in this work, the flow rate of O_2 is chosen 10 sccm to get desired etching rate. From this experiments we can concluded that by decreasing pressure to 10 mTorr and adding low concentration of oxygen, the anisotropic micro-pit arrays with 120 nm depth and surface roughness less than 3 nm could be obtained.

CONCLUSION

We have demonstrated the effect of O_2 addition on SF_6 plasma etching of Si micro-pits etching. The results suggest O_2 etchant and pressure to be the principal factors influencing etching profile. Based on these findings, etching of micro-pits with O_2 addition results a vertical sidewall with less than 3 nm roughness of the inter-pit spacing, while V-groove shaped sidewall is obtained in absence of O_2. The etching process recipes were developed to achieve anisotropic profiles for fabricating vertical sidewalls of Si micro-pits.

REFERENCES

[1] D. Sinton, R. Gordon, AG. Brolo, *Microfluidics and Nanofluidics* **4** (2008) 107-116
[2] C.H. Liu, M.H. Hong, M.C. Lum, H. Flotow, F. Ghadessy, J.B. Zhang, *Appl Phys A* **101** (2010) 237-241.
[3] T. Baba, N. Kamizawa, M. Ikeda, *Physica B* **227** (1996) 415-418
[4] Y. Xu, H.B. Sun, J.Y. Ye, S. Matsuo, H. Misawa, *J. Opt. Soc. Am. B* **18** (2001) 1084-1091
[5] W. Hattori, H. Someya, M. Baba, H. Kawaura, *Journal of Chromatography A* **1051** (2004) 141-146
[6] Y. Huang, B. Agrawal, D. Sun, J.S. Kuo, J.C. Williams, *Biomicrofluidics* **5** (2011) 013412
[7] D. Erickson, S. Mandal, A.H.J. Yang, B. Cordovez, *Microfluid Nanofluid* **4** (2008) 35
[8] X.M. Yan, S. Kwon, A.M. Contreras, M.M. Koebel, J Bokor, G A Somorjai, *Catal. Lett.* **105** (2005) 127
[9] R.R.A Syms, D.F. Moore, *Materials Today* **5** (7) (2002) 26-35
[10] R.R.A. Syms, *J Micromech Microeng* **12** (2002) 211-218
[11] A.J. Watts, W.J.Varhue, *J. Vac. Sci. Technol. A* **10** (1992) 1313
[12] Y. Lii, J. Jorne, *J. Electrochem. Soc.* 137 (1990) 3633
[13] E. Gogolides, H.H. Sawin, *J. Electrochem. Soc.* 136 (1989) 1147-1154
[14] G.S. May, J. Huang, C.J. Spanos, *IEEE Trans. Semicond. Manuf.* 4 (1991) 83-98
[15] I. W. Rangelow, A. Fichelscher, *Proc. SPIE* 1392 (1990) 240
[16] C.P.D. D'Emie, K.K. Chan, J. Blum, *J Vac Scl Technol B* 10 (1992) 1105-1110
[17] M. Francou, J.S. Danel, L. Peccoud, *Sens Actuators Phys A* 46–47 (1995) 17-21
[18] D.M. Manos, D.L. Flamm, Plasma, Etching: An Introduction. Academic Press, Boston, London (1989)
[19] T. Syau, B.J. Baliga, R.W. Hamaker, *J Electrochem Soc* 138 (1991) 3076-3081.

[20] R. Legtenberg, H. Jansen, M. Deboer, M. Elwenspoek, *J Electrochem Soc* 142 (1995) 2020-2028
[21] M. Zeuner, J. Meichsner, H.U. Poll, *Plasma Sources Sci. Technol. 4* (1995) 406-415